Combination Treatment with Histone Deacetylase and Carbonic Anhydrase 9 Inhibitors Shows Therapeutic Potential in Experimental Diffuse Intrinsic Pontine Glioma

Naohide Fujita
The Hospital for Sick Children
Andrew Bondoc
The Hospital for Sick Children
Joji Ishida
The Hospital for Sick Children
Michael S. Taccone
The Hospital for Sick Children
Alexandra Riemenshneider
The Hospital for Sick Children
Amanda Luck
The Hospital for Sick Children
Dilakshan Srikanthan
The Hospital for Sick Children
Robert Siddaway
The Hospital for Sick Children
Akihide Kondo
Juntendo University School of Medicine
Hajime Arai
Juntendo University School of Medicine
Christian Smith
The Hospital for Sick Children
Paul McDonald
BC Cancer Research Institute
Cynthia Hawkins
The Hospital for Sick Children
Shoukat Dedhar
BC Cancer Research Institute
James Rutka (james.rutka@sickkids.ca)
The Hospital for Sick Children

Research Article

Keywords: CA9, SLC-0111, HDAC inhibitor, pyroxamide, combination therapy, DIPG

Posted Date: March 10th, 2022

DOI: https://doi.org/10.21203/rs.3.rs-1427931/v1

Abstract

Purpose: Despite extensive research, an effective and safe treatment for diffuse intrinsic pontine glioma (DIPG) has not been established. In this study, we investigate the therapeutic potential of combination therapy with histone deacetylase (HDAC) and carbonic anhydrase 9 (CA9) inhibitors against DIPG.

Methods: We used RNA sequencing data from DIPG patient samples to evaluate the expression of the carbonic anhydrase family and the activity of the hypoxia signaling pathway. Next, we performed a synergy screen using CA9 inhibitor SLC-0111 and the HDAC inhibitors panobinostat, vorinostat, entinostat, and pyroxamide. We selected the SLC-0111/HDACi combination showing the highest synergy, and its effects on cell proliferation, invasion, and migration were evaluated. We also measured changes in histone acetylation, apoptosis, cell cycle, and intracellular pH.

Results: CA9 was significantly upregulated in human DIPG samples. Furthermore, pathways downstream of CA9 were found to be activated when compared to normal brain tissue. The synergy screen revealed that the combination of SLC-0111 and pyroxamide was most effective at inhibiting DIPG cell proliferation. Furthermore, this combination reduced cell migration and invasion potential while enhancing histone acetylation with subsequent reduction of cell population in S Phase. Finally, the SLC-0111 and pyroxamide combination showed greater reduction of intracellular pH as compared to each agent alone.

Conclusion: Our *in vitro* data suggest that the combination of SLC-0111 and pyroxamide shows promise in the treatment of experimental DIPG. Based on these findings, further investigation of this combination therapy in preclinical models is warranted.

Introduction

Diffuse intrinsic pontine glioma (DIPG) is a brain tumor affecting children between the ages of 6 and 9 [1] and is universally fatal with a median overall survival of only 11 months from diagnosis [2]. Current treatment consists of conventional fractionated radiation therapy which only prolongs overall survival by an average of three months [3]. Efforts to find effective therapies for DIPG have resulted in the discovery of many promising compounds at the preclinical stage; however, it is essential to understand the genetic mechanisms underlying DIPG tumor formation and growth to ensure optimal tumor targeting, drug efficacy, and drug delivery.

The tumor microenvironment has been recognized as an important contributor to tumorigenesis. Tumor cells can alter their own metabolism as well as the metabolism of normal cells in their immediate milieu [4]. To meet the energy needs of rapid cell proliferation, tumor cells utilize aerobic glycolysis, resulting in the accumulation of lactic acid, carbonic acid, and other reactive oxygen species [5]. Cancer cells can increase the expression of monocarboxylate transporters and proton flux regulators to extrude excess protons and avoid acidic stress. Such regulators include the carbonic anhydrases, a large family of zinc metalloenzymes that catalyze the reversible conversion of carbon dioxide to bicarbonate and protons [6].

Carbonic anhydrase 9 (CA9) maintains pH balance in gastrointestinal cells, and its expression is normally restricted to these cells in healthy individuals [7]. However, CA9 has also been shown to be overexpressed in various solid cancers [8], and high CA9 expression correlates with poor prognosis in many types of tumors, including glioblastoma (GBM) [9, 10]. Because of its limited expression in normal cells and specific overexpression in tumor cells, CA9 is an attractive cancer therapy target [11]. In brain tumors, high CA9 expression has been confirmed in glioma, meningioma, and metastatic tumors [12]. In GBM, the CA9 inhibitor SLC-0111 demonstrated effective inhibition of tumor growth *in vivo* [13]. To date, the effects of CA9 inhibition in DIPG is unknown.

DIPG is currently defined as a diffuse midline glioma characterized by high prevalence of specific mutations in the histone H3 gene, specifically *HIST1H3B* H3K27M or *H3F3A* H3K27M. These mutations—lysine-to-methionine substitutions at position 27—induce a loss of methylation and result in aberrant transcription and tumorigenesis [14, 15]. Although these mutations are key drivers in DIPG formation, their functional role remains unclear, thus making them an active area of investigation. Histone deacetylase (HDAC) inhibitors, a class of anti-cancer drugs targeting histone modification, have shown great promise. While effective against many types of tumors, recent reports indicate HDAC inhibitors exhibit increased efficacy when used in combination with other drugs suggesting additive or synergistic effects between the two agents [16, 17]. Calorini et al. utilized the combination of the HDAC inhibitor vorinostat and CA9 inhibitor SLC-0111, demonstrating significant anti-tumor effects in melanoma, colorectal, and breast cancer cell lines [17]. This suggests that the combination of CA9 and HDAC inhibitors is a potential therapeutic strategy. As of yet, this combination has not been studied in brain tumors.

Herein, we evaluate the anti-tumor effects of combination therapy with HDAC and CA9 inhibitors in DIPG cell lines. We analyzed the expression of CA9 and CA9-related signaling pathways in human DIPG samples using RNA sequencing data, and confirmed CA9 pathway overexpression as a potential target for DIPG treatment. We then performed a drug synergy screen with multiple HDAC inhibitors in combination with SLC-0111 in DIPG patient-derived cell lines. Based on the result of this screen, we selected the HDAC1 inhibitor pyroxamide for subsequent experiments as it showed the highest synergistic effect. Through proliferation, invasion, and migration assays, we found that SLC-0111 enhanced the anti-tumor effect induced by pyroxamide. We also measured the extent to which SLC-0111 affects histone acetylation, apoptosis, cell cycle, and intracellular pH (pHi) through western blotting, cell cycle analysis, and pH measurement assay. Our data suggest the combination of CA9 inhibitor SLC-0111 and HDAC inhibitor pyroxamide is a promising novel treatment strategy for DIPG.

Materials And Methods

RNA sequencing analysis

We used human RNA-seq data available on the European Genomics Archive, accession number EGAD00001006450 (https://ega-archive.org). RNA sequencing data from DIPG and normal brain tissue

were generated as previously reported [18]. Gene expression was counted with HTSeq [19], and differential expression was calculated with edgeR [20]. Genes with absolute fold-change > 1 and Benjamini-Hochberg adjusted p-value < 0.05 were classified as differentially expressed. Genes were ranked by multiplying their fold-change sign with the -log10 (adjusted p-value) for pre-ranked gene set enrichment analysis [21].

DIPG cell lines and culture conditions

DIPG cell lines (SU-DIPG-IV, SU-DIPG-VI, SU-DIPG-XVII, and SU-DIPG-XXXVI) were generously provided by Dr. Michelle Monje (Stanford University). Cells were maintained in a 1:1 mixture of Neurobasal-A (Thermo-Fisher Scientific) and DMEM/F12 (Wisent Bioproducts) supplemented with 10mM HEPES, 100μM MEM non-essential amino acids, 1X GlutaMAX-I, 1mM sodium pyruvate (Thermo-Fisher Scientific), 1X antibiotic-antimycotic solution (Wisent BioProducts), 1X B-27 without vitamin A (Gibco), 20ng/ml human epidermal growth factor (Sigma-Aldrich), 20ng/ml human basic fibroblast growth factor (Peprotech), 10ng/ml each human platelet-derived growth factors AA and BB (Shenandoah Biotechnology), 2μg/ml heparin (Stem Cell Technologies) as previously described [22, 23]. Cells were incubated at 37°C in humidified atmosphere containing 5% CO^2 and 21% O^2 (normoxia) or 1% O^2 (hypoxia). Cell lines were validated via DNA fingerprinting using short tandem repeat analysis (The Centre for Applied Genomics, The Hospital for Sick Children).

Synergy screening and cell viability assay

To select a partner drug for CA9 inhibitor SLC-0111, four HDAC inhibitors were used for synergy screening: panobinostat, entinostat, vorinostat (Selleck Chemicals), and pyroxamide (Sigma-Aldrich). SLC-0111 was kindly provided by Welichem Biotech Inc (Vancouver BC, Canada). All drugs were dissolved in DMSO and stored at -80°C until used. Cells were seeded onto 96-well plates at a density of 11,000–20,000 cells/cm^2, with three technical replicates per condition. Cells were allowed to grow for 24 hr, after which drugs were dispensed onto the plate using a D300e Digital Dispenser (Tecan). Preliminary IC50 curves were determined, and in synergy screening, the concentration range for each HDAC inhibitor was set to cover as wide a range as possible around the IC50. These ranges were adjusted for each cell line due to their different sensitivity to each drug. The SLC-0111 concentration range was 2-200μM for all lines. Cells were incubated with drugs under normoxic condition for 72 hr, after which AlamarBlue cell viability reagent (Invitrogen) was added. Fluorescence at 590nm was measured using a VersaMax 190 plate reader (Molecular Devices). IC50 curves were generated using the Boltzmann algorithm in Prism 9.0 (GraphPad Software). Synergy scores were calculated with the Bliss method through SynergyFinder 2.0 whereby scores of 10 or higher were defined as synergistic [24].

Scratch wound assay

Fifty thousand SU-DIPG-IV cells were seeded into each well of an Incucyte Imagelock plate (Sartorius) coated with Matrigel (Corning) as per manufacturer's instructions. After incubation at 37°C for 24 hr, scratch wounds were made with a WoundMaker Tool (Sartorius). Upon confirming successful wounding, 150μl of drug-containing medium was added to migration assay wells, while 50μl of drug-containing

Matrigel and 100µl of drug-containing medium were added to invasion assay wells. Plates were incubated under normoxia or hypoxia and imaged using an Incucyte S3 Live-Cell Analysis System (Sartorius) for 3 days, after which the confluency of each wound was measured using the instrument's software.

Western blotting

DIPG cells were harvested at 80–90% confluence. To check CA9 protein expression, cells were incubated in normoxic or hypoxic conditions for 3 days before harvest. To measure drug effects, cells were treated with 0 or 5µM pyroxamide and 0 or 100µM SLC-0111 for 3 days under normoxia. Cells were washed with ice-cold PBS and lysed in SDS lysis buffer (20mM Tris, 20mM EDTA, 2% SDS, 20% glycerol) containing protease inhibitor cocktail (Roche). Protein concentrations were measured using the DC Protein Assay (Bio-Rad). Equal amounts of protein (20µg) were loaded onto 10% tris-glycine polyacrylamide gels and run at 80Vfor 2 hr. Fractionated proteins were transferred to PVDF membranes using the Trans-Blot Turbo Semi-Dry system (Bio-Rad). Membranes were blocked for 1 hr at room temperature in either 5% BSA or 5% skimmed milk in TBS containing 0.1% Tween-80. Blots were probed with primary antibody in block buffer overnight at 4°C. The primary antibodies used were: anti-CA9 (Novus Biologicals NB100-417, 1:1000), anti-poly ADP-ribose polymerase (Cell Signaling #9542, 1:2000), anti-cleaved caspase 3 (Cell Signaling #9661, 1:1000), anti-p21 (Cell Signaling #2947, 1:2000), anti-acetyl-histone 3 (Sigma-Aldrich 06-599, 1:2000), anti-acetyl-histone 4 (Sigma-Aldrich 06-866, 1:1000), and anti-GAPDH (Cell Signaling #14C10, 1:10000). Subsequently, membranes were incubated at room temperature for one hr with HRP-conjugated secondary antibody (Cell Signaling #58298, 1:10000). Proteins were visualized using enhanced chemiluminescence substrate (PerkinElmer) on a Chemi-Doc MP system (Bio-Rad).

Cell cycle analysis

Cell cycle distribution was analyzed via propidium iodide (PI) staining. Cells were treated in each condition for 48 hr, followed by fixation with 80% ethanol at 4°C overnight. Fixed cells were treated with 2mg/ml RNase A solution (Qiagen) for 5 minutes and stained with 0.1mg/ml PI (Thermo-Fisher Scientific) in 0.1% Triton X-100 (Sigma-Aldrich) in the dark at room temperature for 30 min. Stained cells were filtered through a 40µm mesh and analyzed on an LSRII flow cytometer (Becton Dickinson). Experiments were repeated in triplicate, and raw data was analyzed using FlowJo 10 (Becton Dickinson).

Intracellular pH measurement

pHi was measured using a fluorometric intracellular pH assay kit (Sigma-Aldrich MAK150) following manufacturer's instructions. SU-DIPG-IV cells were seeded onto 96-well plates at 40,000 cells/well and incubated for 24 hr. The medium was replaced with 50µl BCFL-AM dye loading solution containing 5mM Probenecid and incubated at 37°C for 30 min. Compounds in HBSS were administrated and incubated for 15 min. Fluorimetry was carried out at 490nm excitation and 535nm emission wavelengths using a VersaMax 190 plate reader.

Statistical analysis

Data was analyzed using one-way ANOVA with Tukey's post-hoc test via Rstudio. Synergy maps were generated in SynergyFinder 2.0 [24], and figures were created using Prism 9 (GraphPad Software).

Results

CA9 gene, as well as hypoxia, epithelial-mesenchymal transition, and glycolysis pathways, are upregulated in DIPG

Given that carbonic anhydrases are elevated in GBM and their inhibition blocks tumor growth *in vivo*, we analyzed the expression patterns of carbonic anhydrase genes in human DIPG samples using RNA-seq datasets [18]. In the DIPG samples, CA1, 3, 6, 9, 12, 13, 14 were found to be significantly upregulated, and CA4, 7, 10, 11 were significantly downregulated compared to normal brain (Fig. 1a, b, **and Supplementary data 1**). Notably, both CA9 and CA12, the target genes of SLC-0111, were upregulated. No significant differences were found in CA2, 5, 8, 15. We also analyzed the CA9-related gene sets of hypoxia, epithelial-mesenchymal transition (EMT), and glycolysis. Gene set enrichment analysis (GSEA) revealed that all three pathways were significantly upregulated in DIPG (Fig. 1c). As with GBM, these data suggest that CA9 is a potential target for chemotherapy in DIPG [13, 17].

Hypoxia induces CA9 expression in DIPG cell lines

We performed western blot analysis to measure CA9 protein expression in four DIPG cell lines (Fig. 1d). CA9 was not detected under normoxia; however, all four lines showed significant CA9 expression 72 hr after hypoxic conditions were initiated. Previous experiments from our group showed that the DIPG line, SU-DIPG-XIII, does not express CA9 even under hypoxia (data not shown), and was not included in the current study.

Pyroxamide exhibits synergy with SLC-0111 in all DIPG cell lines

Prior to synergy screening, we determined the IC50 for each drug (Fig. 2a, b, **and Supplementary Fig. 1**). The IC50s of SLC-0111 and HDAC inhibitors panobinostat, entinostat, vorinostat, and pyroxamide ranged from approximately 180–300, 0.014–0.02, 0.50–1.45, 0.40–1.10, and 2–5μM respectively, due to variable sensitivity in each cell line (**Supplementary Data 1**). Notably, SLC-0111 did not suppress cell proliferation at concentrations less than 100μM.

After determining the IC50s, we performed synergy screening to determine if HDAC inhibitors synergize with SLC-0111. The summary of this screening is shown in Table 1. Each value represents the synergy score of the most synergistic region in the evaluated range. Pyroxamide showed the highest synergistic effect, particularly in the range of 50–150μM SLC-0111 and 3–10μM pyroxamide, in SU-DIPG-VI, XVII, and XXXVI (Fig. 2c, d **and Supplementary Fig. 2**). In SU-DIPG-IV, synergy occurred in the lower concentration range. Entinostat and vorinostat also showed synergy in SU-DIPG-IV and VI respectively, while panobinostat did not show synergy in any of the cell lines (Table 1). Since pyroxamide consistently

demonstrated higher synergy scores, we selected the combination of pyroxamide and SLC-0111 for subsequent experiments.

Table 1
Bliss synergy scores at most synergistic area

	SU-DIPG-IV	SU-DIPG-VI	SU-DIPG-XVII	SU-DIPG-XXXVI
Panobinostat	8.181	2.886	6.538	0.298
Entinostat	12.717	3.942	7.354	-0.768
Vorinostat	6.725	11.312	5.701	0.017
Pyroxamide	10.237	21.37	13.702	18.693

We next sought to compare the proliferation rates of DIPG cell lines under treatment, specifically using 0, 5, or 10μM pyroxamide and/or 0 or 100μM SLC-0111. Single agent treatment with either drug significantly inhibited proliferation—except for SLC-0111 in SU-DIPG-VI and XVII, which did not show a difference (Fig. 2e **and f**). Combination treatment with SLC-0111 and pyroxamide resulted in significant inhibition of proliferation when compared to pyroxamide alone at both 5μM and 10μM.

Combination treatment inhibits cell invasion and migration

We evaluated the effect of combination drug therapy on the invasion and migration of SU-DIPG-IV using the scratch wound assay (Fig. 3). Under normoxia, treatment with 100μM SLC-0111 alone significantly inhibited invasion and had a greater effect than 5μM pyroxamide alone (Fig. 3a **and c**). Importantly, combination treatment regimens showed a significantly greater inhibitory effect when compared to the respective single agent treatments. Moreover, in hypoxic conditions—considered to be representative of the original tumor environment—the inhibitory effects of both single and combination treatments were enhanced. This combination treatment also showed the most effective inhibition of cell migration; however, the effects were not as profound under normoxia, especially with single treatment (Fig. 3b **and d**). Under hypoxic conditions, as with the invasion assay, the inhibitory effects on cell migration were enhanced in all treatment groups. These results suggest that combination therapy with SLC-0111 and pyroxamide can restrain cell invasion and migration in DIPG cells.

SLC-0111 enhances the cell cycle arrest induced by pyroxamide

To elucidate any alterations in cell cycle following drug treatment, we performed cell cycle analysis using propidium iodide staining (Fig. 4a). SLC-0111 single treatment resulted in a significantly higher population of SU-DIPG-IV cells in the G1 phase compared to control; interestingly, this was not observed in the other cell lines. Furthermore, pyroxamide shifted the cell cycle from the S phase to the G1 phase in all cell lines. Strikingly, combination treatment significantly reduced the S phase population, while also decreasing the G1 population and increasing the G2 population. The sub G1 population was also

elevated in the combination treatment; this was most evident in SU-DIPG-XVII and SU-DIPG-XXXVI, where the differences were significant.

In short, pyroxamide reduced the S phase cell population and induced cell cycle arrest in DIPG cells. SLC-0111 further enhanced cell cycle arrest and increased the sub G1 phase population indicative of cell apoptosis. However, in terms of cell distribution, SLC-0111 did not enhance the effect of pyroxamide in increasing the G1 population.

SLC-0111 potentiates the effect of pyroxamide on histone acetylation and apoptosis

We sought to determine how the addition of SLC-0111 may affect the histone acetylation and apoptosis response induced by pyroxamide (Fig. 4b). As expected, the HDAC inhibitor pyroxamide increased both acetyl-histone 3 (acH3) and acetyl-histone 4 (acH4) in all cell lines, while SLC-0111 only slightly increased these markers in SU-DIPG-IV and SU-DIPG-XXXVI. However, in all cell lines, SLC-0111 enhanced the effect of pyroxamide, resulting in substantially increased levels of acH3 and acH4. We also evaluated apoptosis by measuring levels of poly ADP-ribose polymerase (PARP) and cleaved caspase 3. When treated with SLC-0111 alone, cleaved PARP and cleaved caspase 3 slightly increased in SU-DIPG-VI and XVII, respectively. Single drug treatment with pyroxamide showed an increase in cleaved PARP and cleaved caspase 3, but only a slight increase was observed in SU-DIPG-XVII. In contrast, upon combination therapy, all cell lines showed robust expression of both cleaved PARP and cleaved caspase 3. Additionally, we measured expression of the cyclin-dependent kinase inhibitor p21, a downstream surrogate marker of pyroxamide activity [25, 26]. Indeed, pyroxamide increased p21 levels in our DIPG cell lines; however, in combination with SLC-0111, p21 was unexpectedly attenuated in all lines except SU-DIPG-XXXVI. Taken together, we have shown that pyroxamide increases acetylated histones and induces apoptosis, and the addition of SLC-0111 enhances these effects.

Combination treatment with SLC-0111 and pyroxamide reduces intracellular pH

Finally, we compared pHi between the treatment groups to investigate how pyroxamide may affect the action of SLC-0111 (Fig. 4c). Neither 100μM SLC-0111 nor 5μM pyroxamide alone caused any significant changes in pHi. However, when used in combination, the drugs elicited a significant reduction in pHi as compared to control. These results suggest that SLC-0111 and pyroxamide may enhance each other's effect on pHi.

Discussion

Numerous chemotherapeutic strategies have been attempted previously for patients with DIPG. The classical cytotoxic agents such as cisplatin, cyclophosphamide, carboplatin, etoposide, and vincristine were initially evaluated, but the response rates of children following the use of these drugs were lower than those after conventional radiation therapy [27]. Temozolomide, the current standard

chemotherapeutic treatment for GBM, was also attempted for DIPG patients; unfortunately, it did not improve patient outcomes compared to radiation therapy alone [28]. Molecular-targeted therapies have also been explored—for example, the PDGF/PDGFR inhibitor imatinib, the farnesyl transferase inhibitor tipifarnib, the EGFR inhibitors erlotinib and gefitinib, and VEGFR inhibitor vandetanib [29]—which function to block oncogenic signaling pathways. Unfortunately, these attempts at novel therapeutics have also failed to improve outcome of DIPG patients.

Recently, therapeutic focus has shifted towards targeting epigenetic alterations, the tumor microenvironment, metabolism, and immunomodulation [16, 30]. Accordingly, the epigenetic landscape altered by the H3K27M mutation has been considered as a reasonable target against DIPG, especially since alternative mutations are not found in this tumor [31]. Reagents targeting the epigenetic mechanism, such as H3K27 demethylase inhibitors, enhancer of zeste homologue 2 inhibitors, cyclin-dependent kinase 7 inhibitors, and HDAC inhibitors, have been explored and reported [30]. Among these, HDAC inhibitors showed the most promising effects on decreasing the viability of DIPG cells [32]; indeed, panobinostat and vorinostat are currently undergoing clinical trials as single agents or in combination with other drugs [33–36].

In the current study, we focused on pyroxamide based on the result of synergy screening. Pyroxamide has not been prominently investigated, possibly because it was previously reported to be less effective than other HDAC inhibitors and because it was associated with more side effects [25, 26, 37]. Erythrocytic extramedullary hematopoiesis in the spleen or bone marrow, and splenomegaly have been observed in mice treated with high doses of pyroxamide. Nevertheless, combination with other drugs may reduce the minimum dosage, and thus side effects, of pyroxamide. In our study, pyroxamide exhibited anti-tumor effects most effectively against DIPG cells in combination with the CA9/12 inhibitor, SLC-0111, although its effectiveness and toxicity need to be confirmed *in vivo*. This provides strong rationale for investigating pyroxamide in combination with other drugs.

The mechanism of action by which HDAC inhibitors elicit their effect is still not fully understood; however, various models have been proposed. HDAC inhibitors can affect cell cycle arrest, apoptosis, autophagy, non-coding RNA, cell differentiation via extracellular signal-regulated kinase pathways, anti-angiogenesis, and immunomodulation [38]. In terms of HDAC inhibitors' effects on apoptosis, the p21 and p53 genes have been the focus of prior investigations [39, 40]. Treatment with HDAC inhibitors releases HDAC1 from Sp1 (Promoter-specific RNA polymerase II transcription factor) and increases p21 expression [39], which mediates cell cycle arrest and apoptosis [41, 42]. HDAC inhibitors also increase the acetylation of the p53 protein, which in turn interacts with p21 [43]; thus, both p21 and acetylated p53 are thought to reflect the effect of HDAC inhibitors. We evaluated p21 in the current study because it is one of the few reported downstream markers of pyroxamide activity [25]. We expect that p21 evaluation could be extrapolated as a downstream biomarker of efficacy of pyroxamide treatment in *in vivo* experiments. However, although the addition of SLC-0111 indeed enhanced histone acetylation, cell cycle arrest, and apoptosis, the expression of p21 decreased in three of four cell lines. The reason for this decrease may be that SLC-0111 itself has some role in weakening p21 expression, or that we did not capture p21 at the optimal time

point in its arc of transient expression [44]. Another compelling explanation might be that p21 acts as an anti-apoptotic to restore balance in the cell cycle, as has been suggested previously [45]. Acetylated p53 may be a good indicator of HDAC inhibitors' efficacy even when combined with SLC-0111 [17]; nonetheless, p21 has also been reported to inhibit the effect of p53 [42]. Further experiments are needed to account for the changes we noted in p21 expression. Taken together, our results suggest that SLC-0111 can enhance the effect of pyroxamide in terms of histone acetylation and apoptosis (Fig. 5); however, the implications of p21 and acetylated p53 expression will need to be reconsidered when attempting to measure the effect of HDAC inhibitors, at least in combination with the CA9 inhibitor, SLC-0111.

The expected result of HDAC inhibitor treatment is to restore the function of the histone. However, HDAC inhibitors can affect a variety of pathways as described above [38]. Due to the universal importance of histone acetylation in normal physiology, it might be challenging to eliminate the possibility of off-target effects [31]. Moreover, HDAC inhibitors have shown anti-tumor effects against H3 wild-type DIPG cells as well as H3K27M cells [46]. This may suggest that the effectiveness of HDAC inhibitors is not specific to the epigenetic landscape of DIPG. Regardless, the efficacy of HDAC inhibitors against DIPG cells has been corroborated in several preclinical studies [32, 46]. Therefore, we still consider HDAC inhibitors to be promising anti-cancer drugs. To fully uncover the potential of HDAC inhibitors, it is important to further elucidate the complex nature of histones themselves, as well as to complete clinical trials that are currently underway [31].

DIPG presents an additional challenge in terms of drug delivery. Unlike other high-grade gliomas such as GBM, many DIPGs do not show gadolinium extravasation under magnetic resonance imaging indicating that the blood-brain barrier (BBB) remains intact in DIPG [47]. The BBB prevents many drugs from reaching the central nervous system, thus making it difficult to treat brain tumors effectively with chemotherapeutic agents. To overcome this problem, molecular, cellular, and physical strategies, including focused ultrasound and convection-enhanced delivery, are being investigated [23, 48]. Despite the promise shown by combination therapy with CA9 and HDAC inhibitors, this drug regimen may need to be augmented with transient focal BBB opening to elicit sufficient effect and avoid systemic toxicity.

CA9 is overexpressed in solid tumors like breast and lung cancer [49]. In brain tumors, upregulation of CA9 has been reported in astrocytoma, oligodendroglioma, meningioma, hemangioblastoma, choroid plexus tumors, and in pediatric brain tumors, ependymoma, medulloblastoma, and primitive neuroectodermal tumors [50]. Importantly, our study is the first report describing CA9 expression in DIPG. Through our RNA sequencing data analysis, we found CA9 to be significantly upregulated in DIPG compared to normal brain tissue. Moreover, the pathways of hypoxia, EMT, and glycolysis, in which CA9 has a major role, were all activated. Although the CA9 inhibitor SLC-0111 did not suppress the proliferation of DIPG cell lines, SLC-0111 single treatment inhibited cell invasion and migration, as has been shown for other tumor types such as breast and pancreatic cancers [9, 51], supporting the rationale for targeting the CA9 gene.

Additionally, our pHi measurements indicate that pyroxamide may also enhance the primary effect of SLC-0111—namely, a lowering of pHi. SLC-0111 did not decrease pHi in our studies possibly because the exposure time to each reagent (15 min) might have been insufficient to see an effect. HDAC inhibitors may indirectly help reduce pHi by suppressing angiogenic pathways and the hypoxia-inducible factor 1 pathway as postulated previously [34]. In summary, CA9 is a valid and encouraging therapeutic target in DIPG. Additionally, pyroxamide and SLC-0111 may mutually reinforce one another (Fig. 5), making the combination of these two drugs a promising strategy against DIPG. Since no other studies focus on carbonic anhydrase inhibition in the context of DIPG, we hope that our findings herein will encourage future investigation into the DIPG microenvironment and hypoxia, ultimately spurring creative new interventions for this devastating disease.

The CA family in mammals is divided into four broad subgroups comprised of several isoforms [52]. Another potentially important finding of note from our study is the significant downregulation of expression of the CA4,7 and 11 in DIPG relative to normal brain. The tissue specific functional roles of these CA isoforms are not well understood, but their significant downregulation may provide clues about DIPG pathophysiology and requires further investigation.

Future studies in this field should evaluate drug response in DIPG samples that have low or no expression of CA9 protein. Our RNA seq data analysis showed high expression of CA9 in DIPG, but on the other hand, there are indeed samples that did not express CA9. Therefore, any proposed benefit described in this study can only be applied to CA9-positive DIPG, and should be further validated in CA9-negative samples. Our study does not take into account the differences in synergy effect that may be seen with SLC-0111 and other HDAC inhibitors.

Conclusion

In this study, we have demonstrated the activation of hypoxic response pathways and CA9 overexpression in human DIPG samples. In addition, the CA9 inhibitor SLC-0111 and pyroxamide exhibit mutual synergy, indicating that this drug combination could be a candidate for novel therapy against DIPG. *In vivo* experimentation in preclinical models, as well as a greater understanding of the histone response itself, will be essential to evaluate the true potential of this therapy. DIPG is a universally fatal and relatively common pediatric brain tumor, stressing the urgent need to establish new and effective treatments. Its refractory nature may also necessitate a multi-drug, multi-modality treatment strategy. We hope that these studies will inspire and drive critical research needed for developing new treatment approaches for DIPG.

Declarations

Acknowledgement

We would like to thank Dr. Emily Reddy (SickKids-UHN Flow Cytometry Facility) for assistance in cell cycle analysis, Cory Richman for assistance in using hypoxic chambers, Kimberly Lau (SickKids Imaging) for assistance with plate reading, and Dr. Chris Fladd (SickKids Proteomics, Analytics, Robotics, and Chemical Biology Centre) for assistance with Incucyte live-cell imaging. SD acknowledges financial support from CIHR Foundation Scheme grant: FDN-143318

Funding

This study was supported by grants from the Canadian Institutes of Health Research (391243 awarded to JTR); Curing Kids Cancer Foundation, The Cure Starts Now, The DIPG Collaborative, Meagan's Hug (Meagan Bebenek Foundation), b.r.a.i.n.child, and the Wiley Fund.

Competing interests

The authors have no conflicts of interest to disclose.

References

1. Panditharatna E et al (2015) Clinicopathology of diffuse intrinsic pontine glioma and its redefined genomic and epigenomic landscape. Cancer Genet 208(7–8):367–373
2. van Veldhuijzen SEM et al (2017) External validation of the diffuse intrinsic pontine glioma survival prediction model: a collaborative report from the International DIPG Registry and the SIOPE DIPG Registry. J Neurooncol 134(1):231–240
3. Kebudi R, Cakir FB (2013) Management of diffuse pontine gliomas in children: recent developments. Paediatr Drugs 15(5):351–362
4. Cairns RA, Harris IS, Mak TW (2011) Regulation of cancer cell metabolism. Nat Rev Cancer 11(2):85–95
5. Riemann A et al (2011) Acidic environment leads to ROS-induced MAPK signaling in cancer cells. PLoS ONE 6(7):e22445
6. van Kuijk SJ et al (2016) Prognostic Significance of Carbonic Anhydrase IX Expression in Cancer Patients: A Meta-Analysis. Front Oncol 6:69
7. Morgan PE et al (2007) Interactions of transmembrane carbonic anhydrase, CAIX, with bicarbonate transporters. Am J Physiol Cell Physiol 293(2):C738–C748
8. Singh S et al (2018) Cancer Drug Development of Carbonic Anhydrase Inhibitors beyond the Active Site.Molecules, 23(5)
9. Lou Y et al (2011) Targeting tumor hypoxia: suppression of breast tumor growth and metastasis by novel carbonic anhydrase IX inhibitors. Cancer Res 71(9):3364–3376
10. Reardon DA et al (2009) Metronomic chemotherapy with daily, oral etoposide plus bevacizumab for recurrent malignant glioma: a phase II study. Br J Cancer 101(12):1986–1994

11. Nocentini A, Supuran CT (2018) Carbonic anhydrase inhibitors as antitumor/antimetastatic agents: a patent review (2008–2018). Expert Opin Ther Pat 28(10):729–740
12. Proescholdt MA et al (2005) Expression of hypoxia-inducible carbonic anhydrases in brain tumors. Neuro Oncol 7(4):465–475
13. Boyd NH et al (2017) Addition of carbonic anhydrase 9 inhibitor SLC-0111 to temozolomide treatment delays glioblastoma growth in vivo. JCI Insight, 2(24)
14. Castel D et al (2015) Histone H3F3A and HIST1H3B K27M mutations define two subgroups of diffuse intrinsic pontine gliomas with different prognosis and phenotypes. Acta Neuropathol 130(6):815–827
15. Meel MH et al (2018) Signaling pathways and mesenchymal transition in pediatric high-grade glioma. Cell Mol Life Sci 75(5):871–887
16. Pal S et al (2018) Dual HDAC and PI3K Inhibition Abrogates NFkappaB- and FOXM1-Mediated DNA Damage Response to Radiosensitize Pediatric High-Grade Gliomas. Cancer Res 78(14):4007–4021
17. Ruzzolini J et al (2020) A potentiated cooperation of carbonic anhydrase IX and histone deacetylase inhibitors against cancer. J Enzyme Inhib Med Chem 35(1):391–397
18. Pajovic S et al (2020) Epigenetic activation of a RAS/MYC axis in H3.3K27M-driven cancer. Nat Commun 11(1):6216
19. Anders S, Pyl PT, Huber W (2015) HTSeq–a Python framework to work with high-throughput sequencing data. Bioinformatics 31(2):166–169
20. Robinson MD, McCarthy DJ, Smyth GK (2010) edgeR: a Bioconductor package for differential expression analysis of digital gene expression data. Bioinformatics 26(1):139–140
21. Subramanian A et al (2005) Gene set enrichment analysis: a knowledge-based approach for interpreting genome-wide expression profiles. Proc Natl Acad Sci U S A 102(43):15545–15550
22. Vinci M et al (2018) Functional diversity and cooperativity between subclonal populations of pediatric glioblastoma and diffuse intrinsic pontine glioma cells. Nat Med 24(8):1204–1215
23. Ishida J et al (2021) MRI-guided focused ultrasound enhances drug delivery in experimental diffuse intrinsic pontine glioma. J Control Release 330:1034–1045
24. Ianevski A et al (2017) SynergyFinder: a web application for analyzing drug combination dose-response matrix data. Bioinformatics 33(15):2413–2415
25. Lisa M, Butler et al (2001) Inhibition of Transformed Cell Growth and Induction of Cellular Differentiation by Pyroxamide, an Inhibitor of Histone Deacetylase. Clin Cancer Reseach 7(4):9
26. Martha C, Kutko et al (2003) Histone Deacetylase Inhibitors Induce Growth Suppression and Cell Death in Human Rhabdomyosarcoma in Vitro. Clin Cancer Reseach 9(15):7
27. Hargrave D, Bartels U, Bouffet E (2006) Diffuse brainstem glioma in children: critical review of clinical trials. Lancet Oncol 7(3):241–248
28. Cohen KJ et al (2011) Temozolomide in the treatment of children with newly diagnosed diffuse intrinsic pontine gliomas: a report from the Children's Oncology Group. Neuro Oncol 13(4):410–416

29. Gwak HS, Park HJ (2017) Developing chemotherapy for diffuse pontine intrinsic gliomas (DIPG). Crit Rev Oncol Hematol 120:111–119
30. Graham MS, Mellinghoff IK, Glioma H-M (2020) : Molecular Mechanisms, Preclinical Models, and Implications for Therapy. Int J Mol Sci, 21(19)
31. Lu VM, Daniels DJ (2021) Epigenetic-Targeted Treatments for H3K27M-Mutant Midline Gliomas. Adv Exp Med Biol 1283:73–84
32. Grasso CS et al (2015) Functionally defined therapeutic targets in diffuse intrinsic pontine glioma. Nat Med 21(6):555–559
33. A Study of Panobinostat in Combination With Everolimus for Children and Young Adults With Gliomas. https://ClinicalTrials.gov/show/NCT03632317
34. Trial of Panobinostat in Children With Diffuse Intrinsic Pontine Glioma. https://ClinicalTrials.gov/show/NCT02717455
35. Vorinostat and Temsirolimus With or Without Radiation Therapy in Treating Younger Patients With Newly Diagnosed or Progressive Diffuse Intrinsic Pontine Glioma. https://ClinicalTrials.gov/show/NCT02420613
36. Vorinostat and Radiation Therapy Followed by Maintenance Therapy With Vorinostat in Treating Younger Patients With Newly Diagnosed Diffuse Intrinsic Pontine Glioma. https://ClinicalTrials.gov/show/NCT01189266
37. Einsiedel HG et al (2006) Histone deacetylase inhibitors have antitumor activity in two NOD/SCID mouse models of B-cell precursor childhood acute lymphoblastic leukemia. Leukemia 20(8):1435–1436
38. Eckschlager T et al (2017) Histone Deacetylase Inhibitors as Anticancer Drugs.Int J Mol Sci, 18(7)
39. Ocker M, Schneider-Stock R (2007) Histone deacetylase inhibitors: signalling towards p21cip1/waf1. Int J Biochem Cell Biol 39(7–8):1367–1374
40. Zhao Y et al (2006) Acetylation of p53 at lysine 373/382 by the histone deacetylase inhibitor depsipeptide induces expression of p21(Waf1/Cip1). Mol Cell Biol 26(7):2782–2790
41. Tetsuo, Suzuki et al (2000) Effect of trichostatin A on cell growth and expression of cell cycle- and apoptosis-related molecules in human gastric and oral carcinoma cell lines. Int J Cancer 88:6
42. Mahyar-Roemer M, Roemer K (2001) p21 Waf1/Cip1 can protect human colon carcinoma cells against p53-dependent and p53-independent apoptosis induced by natural chemopreventive and therapeutic agents. Oncogene 20(26):3387–3398
43. Tang Y et al (2008) Acetylation is indispensable for p53 activation. Cell 133(4):612–626
44. Richon VM et al (2000) Histone deacetylase inhibitor selectively induces p21WAF1 expression and gene-associated histone acetylation. Proc Natl Acad Sci U S A 97(18):10014–10019
45. Janicke RU et al (2007) The multiple battles fought by anti-apoptotic p21. Cell Cycle 6(4):407–413
46. Hennika T et al (2017) Pre-Clinical Study of Panobinostat in Xenograft and Genetically Engineered Murine Diffuse Intrinsic Pontine Glioma Models. PLoS ONE 12(1):e0169485

47. Schroeder KM, Hoeman CM, Becher OJ (2014) Children are not just little adults: recent advances in understanding of diffuse intrinsic pontine glioma biology. Pediatr Res 75(1–2):205–209
48. Arvanitis CD, Ferraro GB, Jain RK (2020) The blood-brain barrier and blood-tumour barrier in brain tumours and metastases. Nat Rev Cancer 20(1):26–41
49. Ciccone V et al (2020) Pharmacological Inhibition of CA-IX Impairs Tumor Cell Proliferation, Migration and Invasiveness.Int J Mol Sci, 21(8)
50. Haapasalo J et al (2020) The Expression of Carbonic Anhydrases II, IX and XII in Brain Tumors.Cancers (Basel), 12(7)
51. McDonald PC et al (2019) Regulation of pH by Carbonic Anhydrase 9 Mediates Survival of Pancreatic Cancer Cells with Activated KRAS in Response to Hypoxia. Gastroenterology 157(3):823–837
52. Breton S The Cellular Physiology of Carbonic Anhydrases. JOP2 (4 suppl): p.159–164

Supplemental Data

Supplementary data 1 file is not available with this version.

Figures

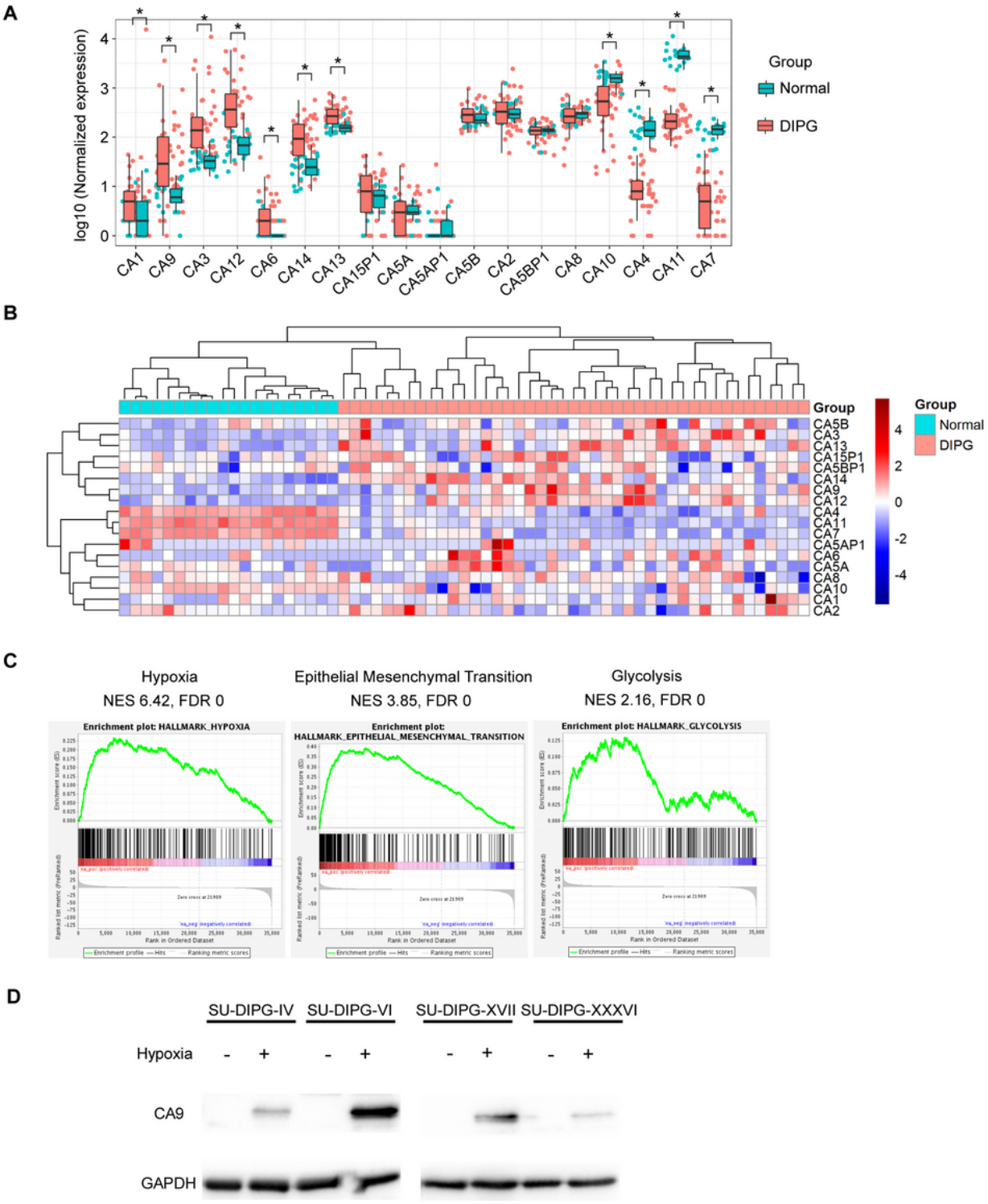

Figure 1

Carbonic anhydrase gene expression in DIPG and the activity of CA9-related pathways. (a) Box-Whisker plot of the differential expression and the variability in relative RNA expression (log10 scale) for carbonic anhydrase genes in 44 DIPG samples and 20 normal brain samples. *$p < 0.05$. (b) Hierarchical clustering of carbonic anhydrase RNA expression in DIPG and normal brain samples. (c) Gene set enrichment analysis of hypoxia, EMT and glycolysis-related genes in human DIPG samples. NES: normalized

enrichment score. FDR: false discovery rate. (d) Western blot for CA9 in four DIPG cell lines treated under normoxia or hypoxia

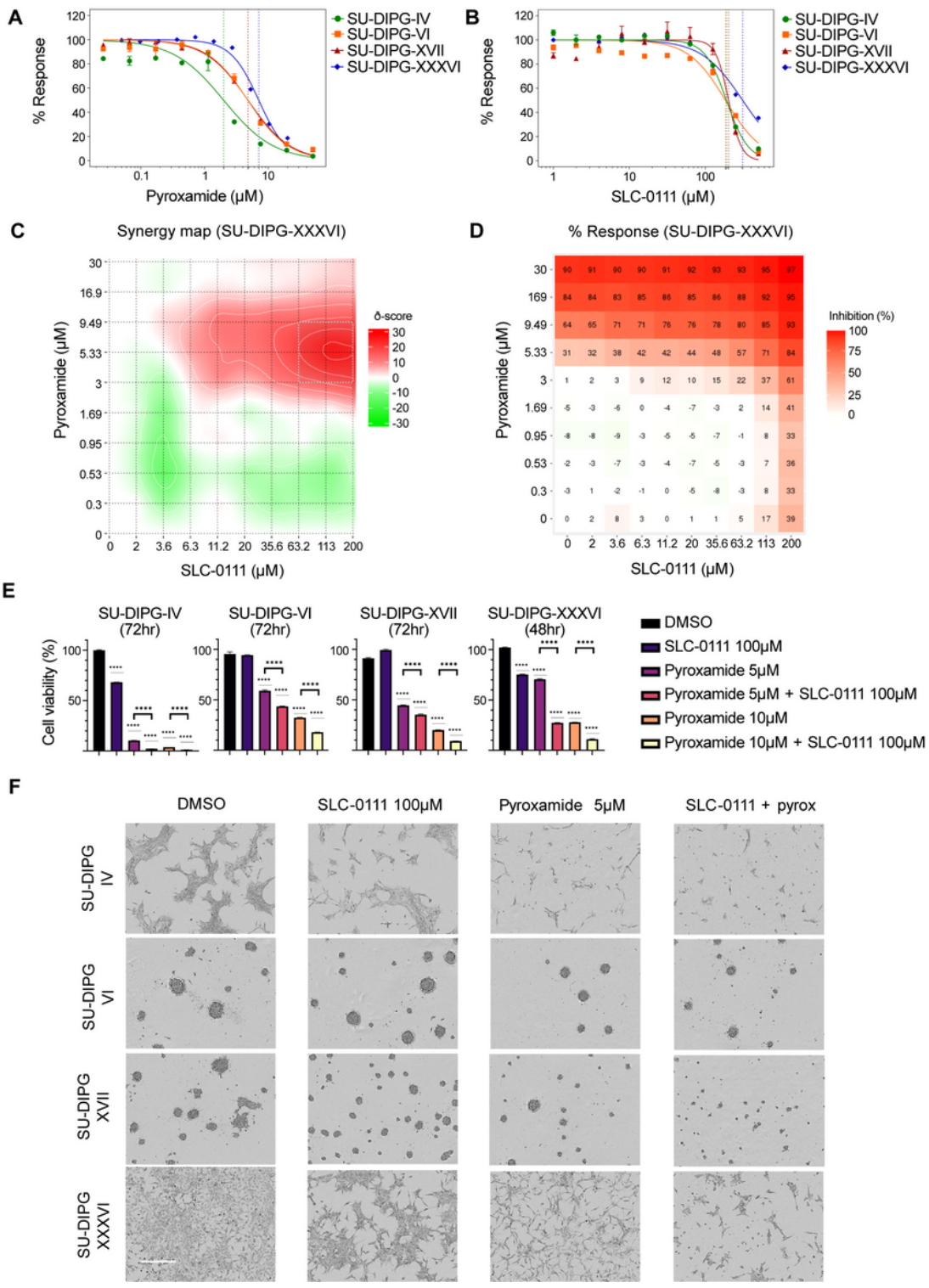

Figure 2

The effect of combination treatment with SLC-0111 and pyroxamide on DIPG cell proliferation. (a, b) IC50 curves of pyroxamide (a) and SLC-0111 (b) in four DIPG cell lines. Dashed lines indicate IC50 value. (c, d)

The representative synergy map and percent response heat map using the Bliss scores for the combination of SLC-0111 and pyroxamide in SU-DIPG-XXXVI. (e) Cell viability after 72h treatment with control (DMSO), 100μM SLC-0111, 5 or 10μM pyroxamide, or a combination of these drugs, as measured by AlamarBlue assay. ****$p < 0.0001$. (f) Micrographs of four DIPG cell lines after 72hr treatments in each condition. Scale bar = 400μm

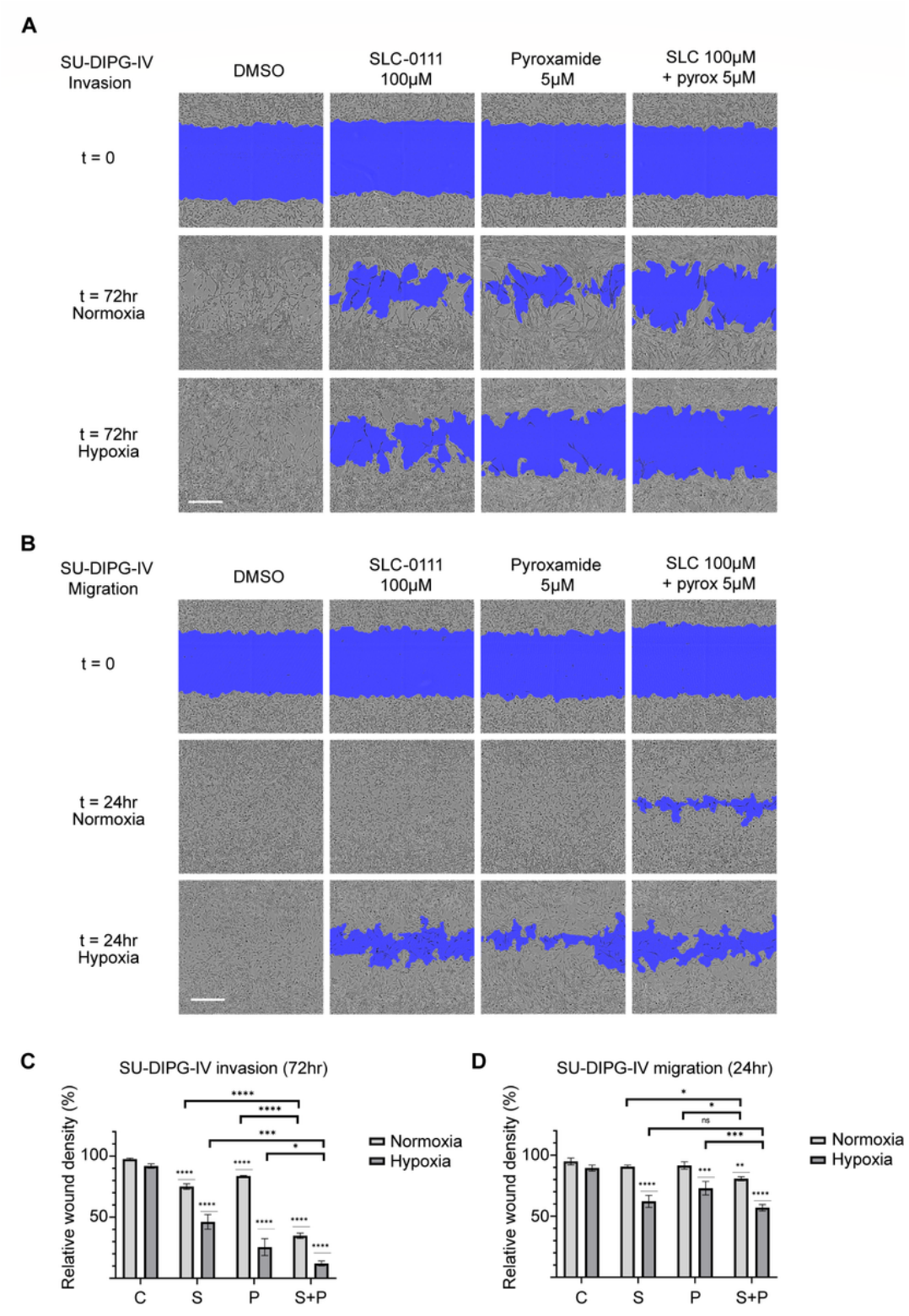

Figure 3

The effect of SLC-0111 and pyroxamide on cell invasion and migration. (a) Representative images of SU-DIPG-IV invasion assay wells at 0 and 72 hr. Blue shading indicates cell-free area. (b) Representative images of SU-DIPG-IV migration assay wells at 0 and 24 hr. Blue shading indicates cell-free area. (c, d) Relative wound density of invasion and migration assay wells at endpoint. C: control (DMSO), S: 100μM SLC-0111, P: 5μM pyroxamide. Scale bars = 400μm, *$p < 0.05$, **$p < 0.01$, ***$p < 0.001$, ****$p < 0.0001$, ns: not significant

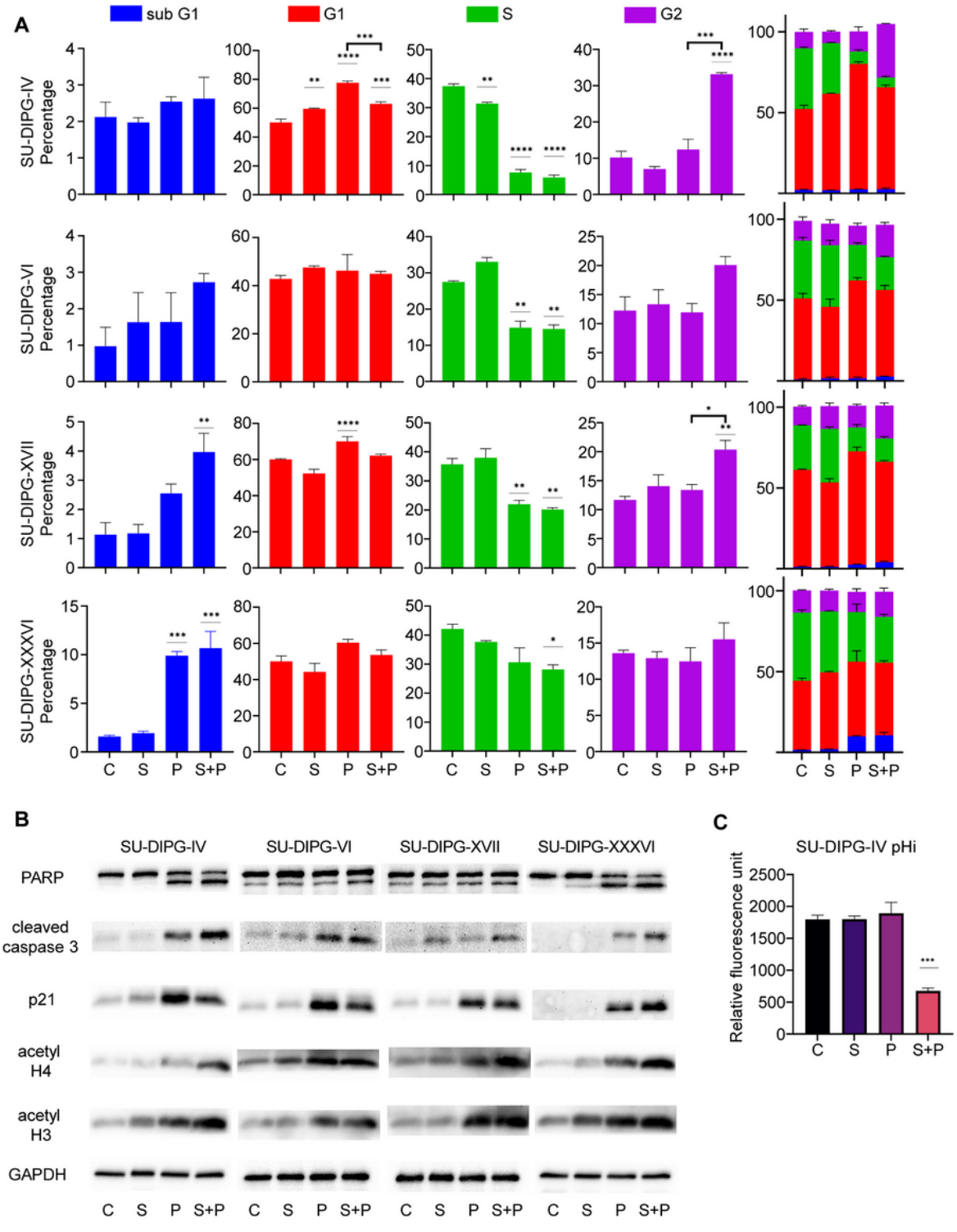

Figure 4

Cell cycle changes resulting from SLC-0111 and pyroxamide treatment. (a) Distribution of SU-DIPG-IV cell populations based on cell cycle phase and stacked bar graphs illustrating cell cycle distribution in all 4 lines. (b) Western blot of PARP, cleaved caspase 3, p21, acetyl H4, and acetyl H3 in DIPG cells treated with SLC-0111 and/or pyroxamide. (c) Intracellular pH as measured by fluorescence intensity. C: control (DMSO), S: 100μM SLC-0111, P: 5μM pyroxamide. *$p < 0.05$, **$p < 0.01$, ***$p < 0.001$, ****$p < 0.0001$

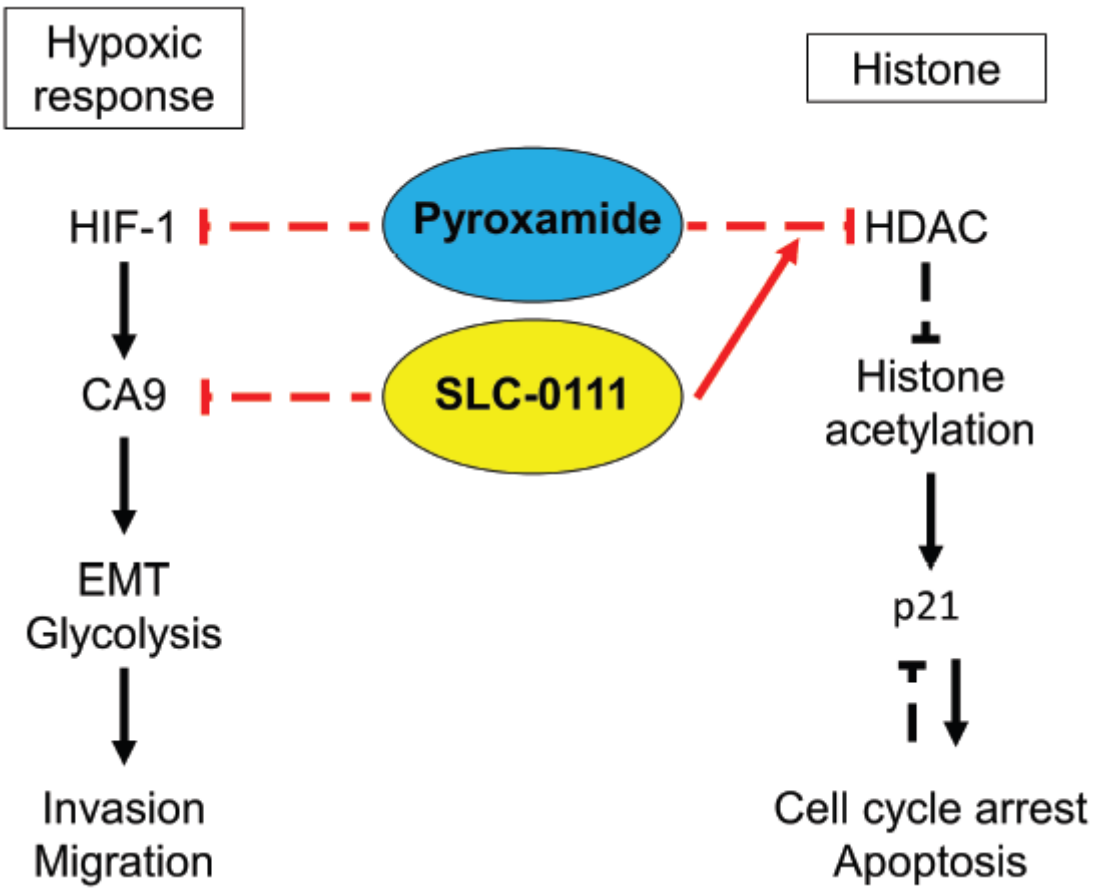

Figure 5

The proposed schema of histone acetylation and hypoxia-related pathway. Pyroxamide inhibits HDAC and induces cell cycle arrest and apoptosis via p21. p21 can receive negative feedback when apoptosis is highly induced. SLC-0111 potentiates the increase of acetylated histone. SLC-0111 inhibits CA9, and pyroxamide can also enhance SLC-0111 by inhibiting the HIF-1 pathway.

Supplementary Files

This is a list of supplementary files associated with this preprint. Click to download.

- SupplementalFigure1.tif

- SupplementalFigure2A.tif
- SupplementalFigure2B.tif
- SupplementalFigure2C.tif
- SupplementalFigure2D.tif